Supplementary Information (SI) for Physical Chemistry Chemical Physics.

Supplementary Information

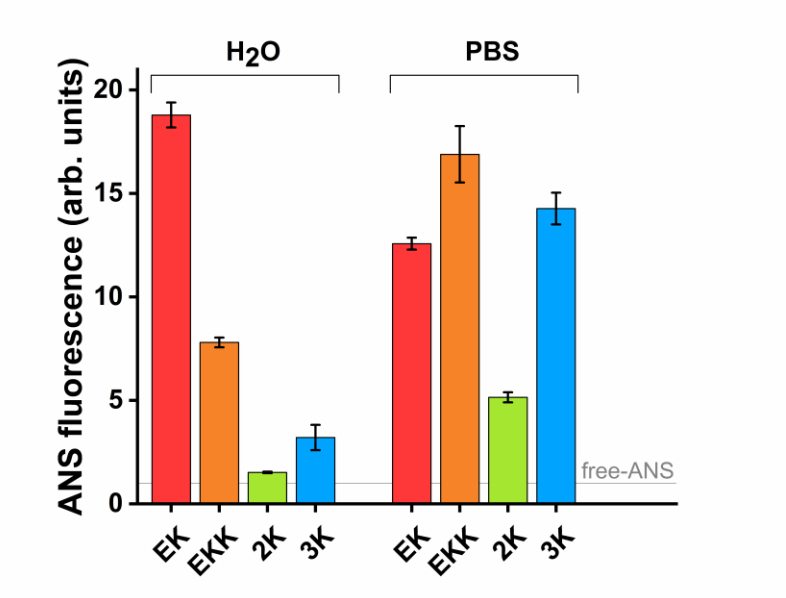

Supplementary Figure 1: ANS binding capacity for different peptides. ANS binding of 125 μM of different peptides in water and PBS using the ANS probe at 2.5 μM. The emission intensities at the maxima were read, and values were normalized for that of unbound ANS. Gray line highlights the reference signal of free ANS. Error bars represent the standard deviation of the mean for three independent experiments.

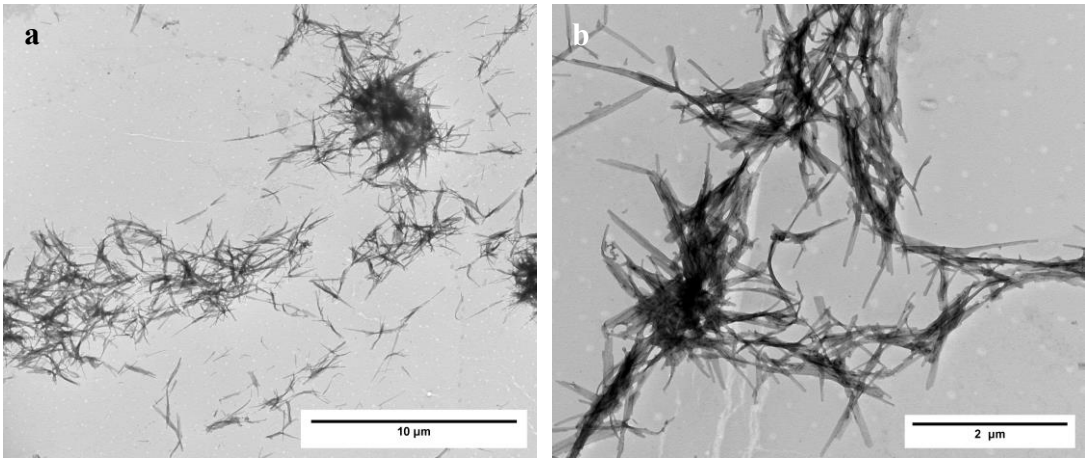

Supplementary Figure 2: Electron micrograph images of EK in PBS (125 µM) showing a) needle-like morphology on micrometer long and b) striped lamellar architecture.

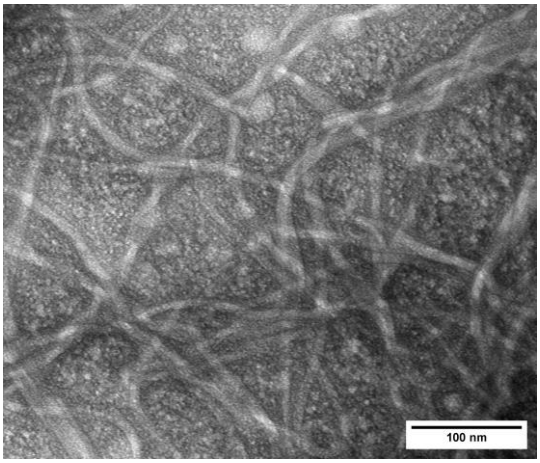

Supplementary Figure 3: Electron micrograph images of EKK (125 µM) in water where elongated twisted fibrils are observed.

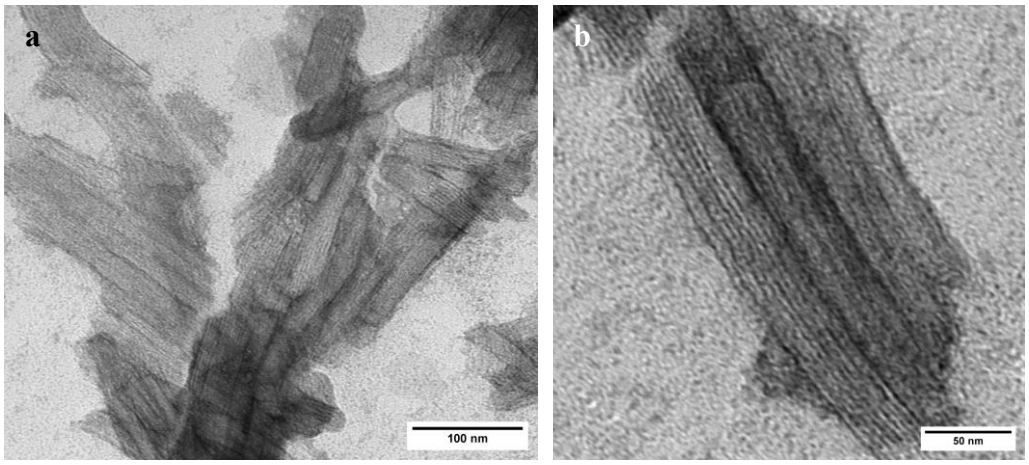

Supplementary Figure 4: Electron micrograph images of EKK (125 μM) in PBS where more packed and striped rectangular lamellae are present such as lamellin-3K.

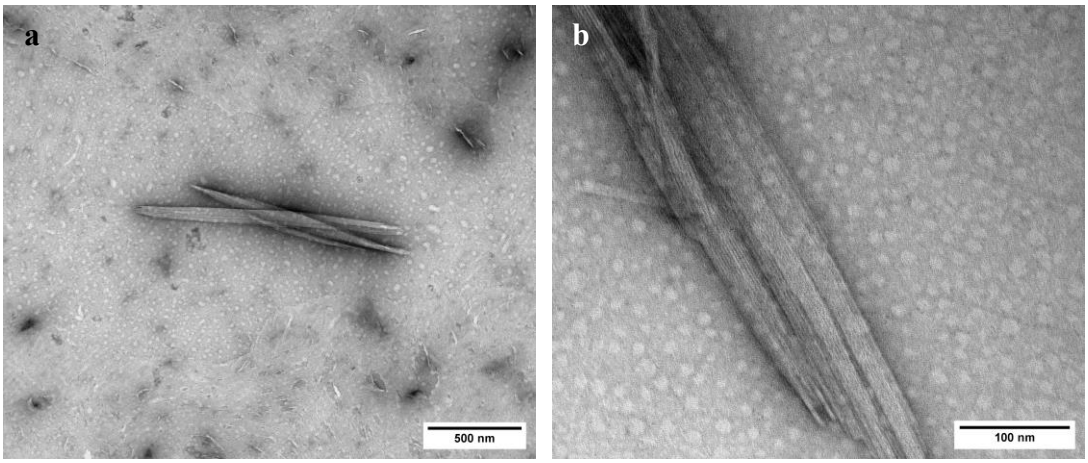

Supplementary Figure 5: Electron micrograph images of 2K (125 μM) in PBS. a) 2K generates (up to micrometer) long, bundled, fibrillary structures, b) The presence of striped morphology is clearly observed.

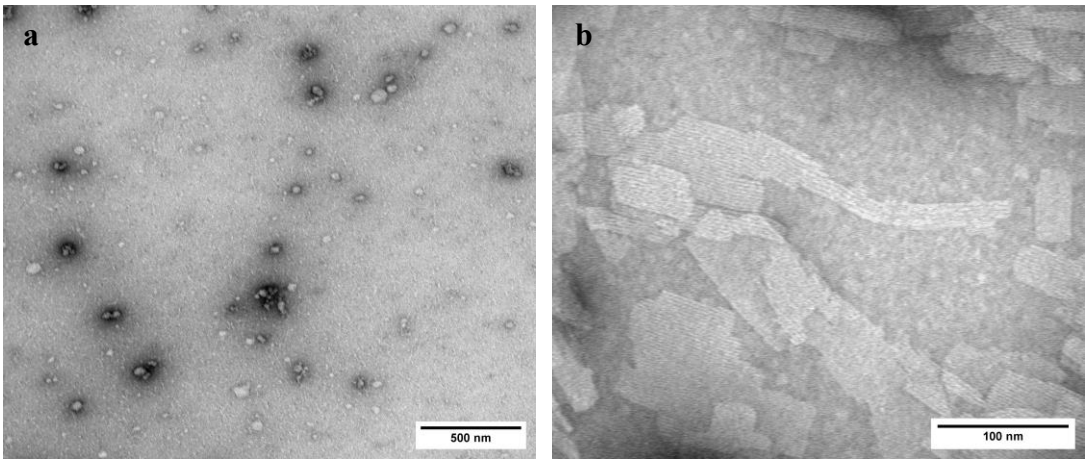

Supplementary Figure 6: Electron micrograph images of 3K (125 μM) in different media. a) in water, 3K forms spherical aggregates, b) 3K in PBS displays shorter, more angular, sheet-like structure also known as lamellin-3K.

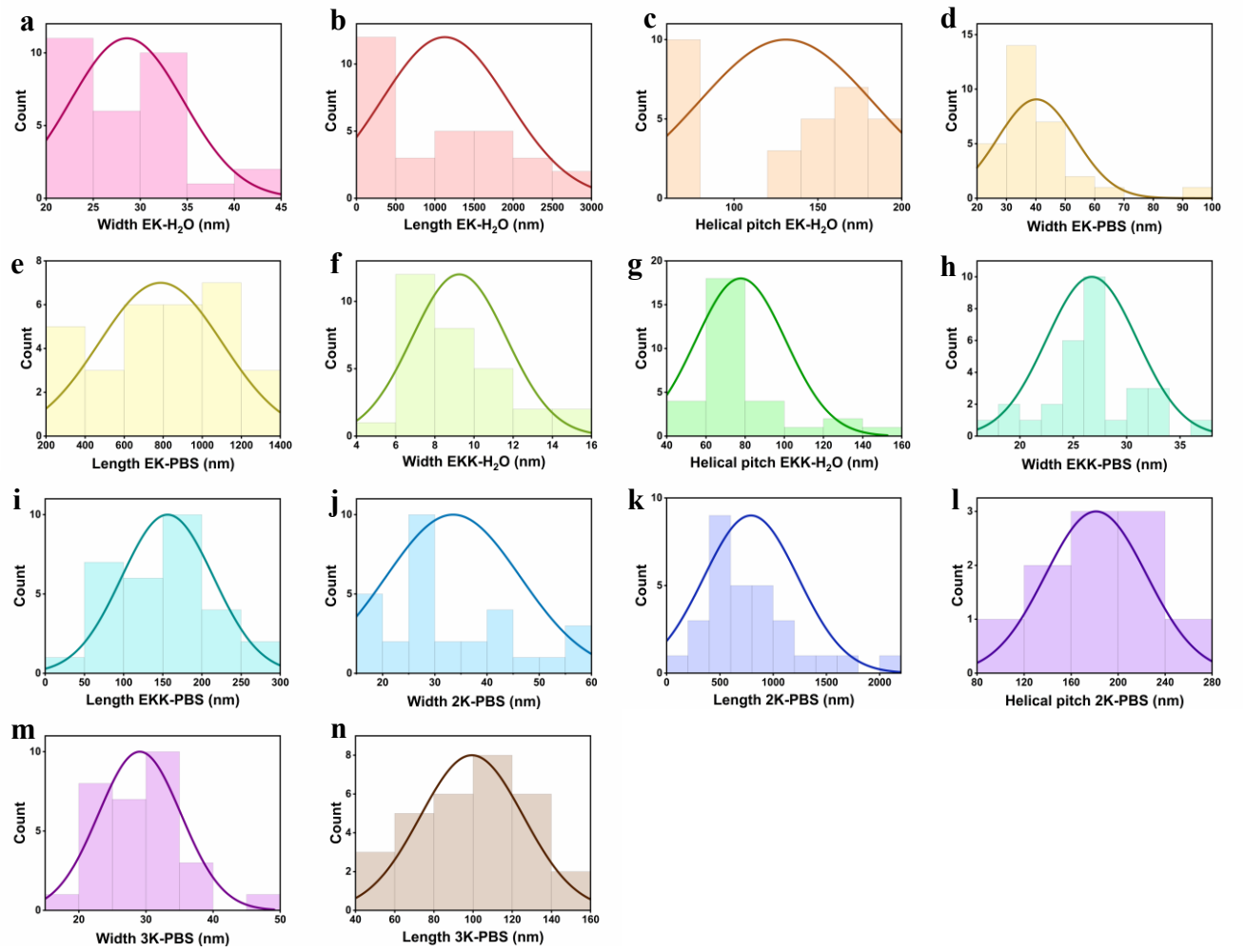

Supplementary Figure 7: Histograms showing the size distribution of the width, length and helical pitch of the four peptides. a-c) EK in water, d) and e) EK in PBS, f) and g) EKK in water, h) and i) EKK in PBS, j-l) 2K in PBS, m) and n) 3K in PBS. Values were determined from TEM images and analyzed with ImageJ software. Distance parameters and the number of objects/particles calculated for each parameter is summarized in Supplementary Table 1.

Supplementary Table 1: Spatial dimensions of the four peptides. Values were calculated from parameters determined based on TEM images using the ImageJ software. The data are represented as mean ± SD where the number of objects analysed are given.

Sample	Parameter	No. of objects	Distance (nm)
EK-H_2O	Width	30	28.59 ± 6.03
EK-H_2O	Length	30	1125.61 ± 808.37
EK-H_2O	Helical pitch	30	130.90 ± 51.87
EK-PBS	Width	30	40.19 ± 13.20
EK-PBS	Length	30	786.84 ± 316.76
EKK-H_2O	Width	30	9.24 ± 2.42
EKK-H_2O	Length	n.a.	Infinite fibrils
EKK-H_2O	Helical pitch	30	77.73 ± 23.02
EKK-PBS	Width	30	26.73 ± 4.25
EKK-PBS	Length	30	156.17 ± 58.66
2K-H_2O	spherical associates		
2K-PBS	Width	30	33.49 ± 12.91
2K-PBS	Length	30	791.34 ± 444.02
2K-PBS*	Helical pitch	10	181.24 ± 43.16
3K-H_2O	spherical aggregates		
3K-PBS	Width	30	29.07 ± 6.15
3K-PBS	Length	30	99.40 ± 26.35

*The helical pitch was observed only in a few instances for 2K in PBS, presenting more a twisted motif.

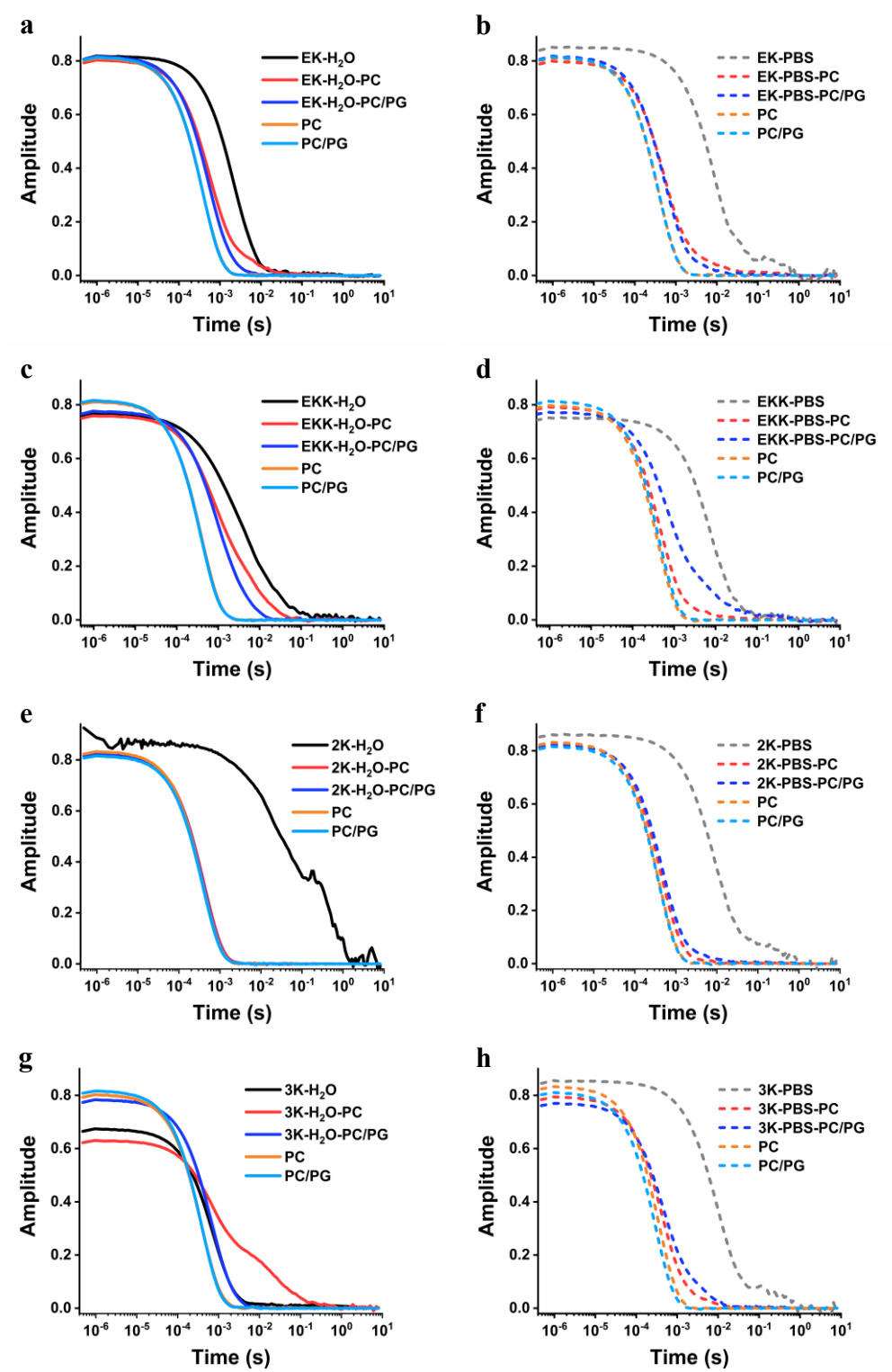

Supplementary Figure 8: Dynamic light scattering of the peptides (125 μM) with liposomes (ratio peptide:liposome, 1:10) in different media. EK in a) water and b) PBS, EKK in c) water and d) PBS, 2K in e) water and f) PBS, 3K in g) water and h) PBS. Peptide binding to the lipids introduced no major changes in the correlation function in case of EK and 2K in both water and PBS (a, b, e and f) as can also be observed from their hydrodynamic diameters given below (Supplementary Table 2). In presence of liposomes in aqueous media, EKK

and 3K, exhibit slight perturbations in the correlation function towards higher decay times which is reflected in their higher hydrodynamic diameters and consistent with formation of aggregates on the liposome surface[1–3] (c and g).

Supplementary Table 2: Dynamic light scattering parameters as obtained from the measurements. PdI represents the polydispersity index.

Media	**Water**			**PBS**		
Sample	Mean hydrodynamic diameter (nm)	PdI (%)	Mass (%)	Mean hydrodynamic diameter (nm)	PdI (%)	Mass (%)
EK	205	31	70	1398	77	100
	647	36	30	-	-	-
EK-PC	99	34	99.9	91	36	99.9
	1143	39	0.1	906	37	0.1
EK- PC/PG	119	29	99.7	10	32	99.8
	828	39	0.3	822	35	0.2
EKK	103	35	96.2	1896	67	100
	683	50	3.8	-	-	-
EKK-PC	156	65	100	95	30	100
EKK- PC/PG	121	41	99.5	98	51	99.9
	916	61	0.5	1296	59	0.1
2K	69	121	99.3	1274	79	100
	1186	122	0.7	-	-	-
2K-PC	109	28	100	99	22	99.9
	-	-	-	761	23	0.1
2K-PC/PG	108	23	100	97	25	100
3K	81	29	55.7	1445	62	100
	197	32	44.3	-	-	-
3K-PC	106	65	100	84	23	100
3K- PC/PG	143	25	98.7	74	26	99.8
	564	29	1.3	865	29	0.2
PC	100	24	100	98	22	100
PC/PG	101	21	100	8	20	100

IR Spectroscopy

To inspect further the peptide-membrane interactions, IR spectroscopy was applied for the analysis, three spectral regions were selected: i) the 3,000 – 2,800 cm^{-1} wavenumber region; this region is dominated by the CH_2 stretching bands of lipid acyl chains; ii) the 1,800 – 1,500 cm^{-1} wavenumber region; here beside the carbonyl stretching at 1,738 cm^{-1} of the phospholipids, the amide I and amide II bands of the peptide can be also followed; iii) the 1,300 – 900 cm^{-1} wavenumber region, where the phosphate bands of the lipid headgroups are dominant.
In water, EKK does not introduce any changes in the acyl region of PC while it does in PC/PG and introduces a shift from 2,924 cm^{-1} to 2,926 cm^{-1} and from 2,854 to 2,855 cm^{-1}, the latter band which is the symmetric stretching vibration band of CH_2 groups of lipid acyl chains, is commonly used to characterize the lipid packing/order in the membrane. A shift towards higher wavenumbers is indicative of a perturbation of the lipid chain packing (Supplementary Figure 9a). In PBS, both PC and PC/PG do not induce any major changes in this region which is in accordance with CD data (Supplementary Figure 9d). Similar slight shifts in spectral intensity is observed for EK and 2K in both water and PBS media indicating interactions with the lipid bilayer which is also in accordance with the CD spectral patterns (Supplementary Figures 10a,d, 11a and d).[4] However, no significant alterations in lipid acyl chain vibrations were observed for 3K (Supplementary Figures 12a and d).
The amide region for 4 peptides in both media and in presence of PC and PC/PG show in different intensity, the bands at ~ 1,689 cm^{-1} and the emergence band at ~ 1,674 cm^{-1} indicating the presence of backbone amide C=O groups not involved as acceptors in H-bonding and the aggregation of peptides in an extended conformation at the lipid surface[1,5] respectively, similar to the carpet model mechanism reported earlier for the membrane activity of antimicrobial peptides[6] (AMP).
In the phosphate region of PC liposome, characteristic bands of PO^{2-} moiety (asymmetric PO^{2-} stretching vibration around 1,245 cm^{-1}, symmetric PO^{2-} stretching vibration around 1,090 cm^{-1}), R-O-P-O-R' stretching of phosphate diester group (around 1,070 cm^{-1}) and the C-N-C stretching of choline group (around 970 cm^{-1}) are present.[7,8] For PC/PG, due to the present of mixed headgroups, the characteristic bands are less featured. In case of EK in both the media, 2K and 3K in water, shifts are observed in the PO^{2-} stretching vibrations which can be attributed to the on-surface localization of these peptides as reported earlier (Supplementary Figures 10c,f, 11c and 12c).[4] However, the invariance of the phosphate and choline vibrations for EKK in both media, 2K and 3K in PBS are due to their pre-formed structure which hinders perturbation of the lipid membrane, commonly observed for peptide-mixed lipid bilayer interactions (Supplementary Figures 9c,f, 11f and 12f).[9]

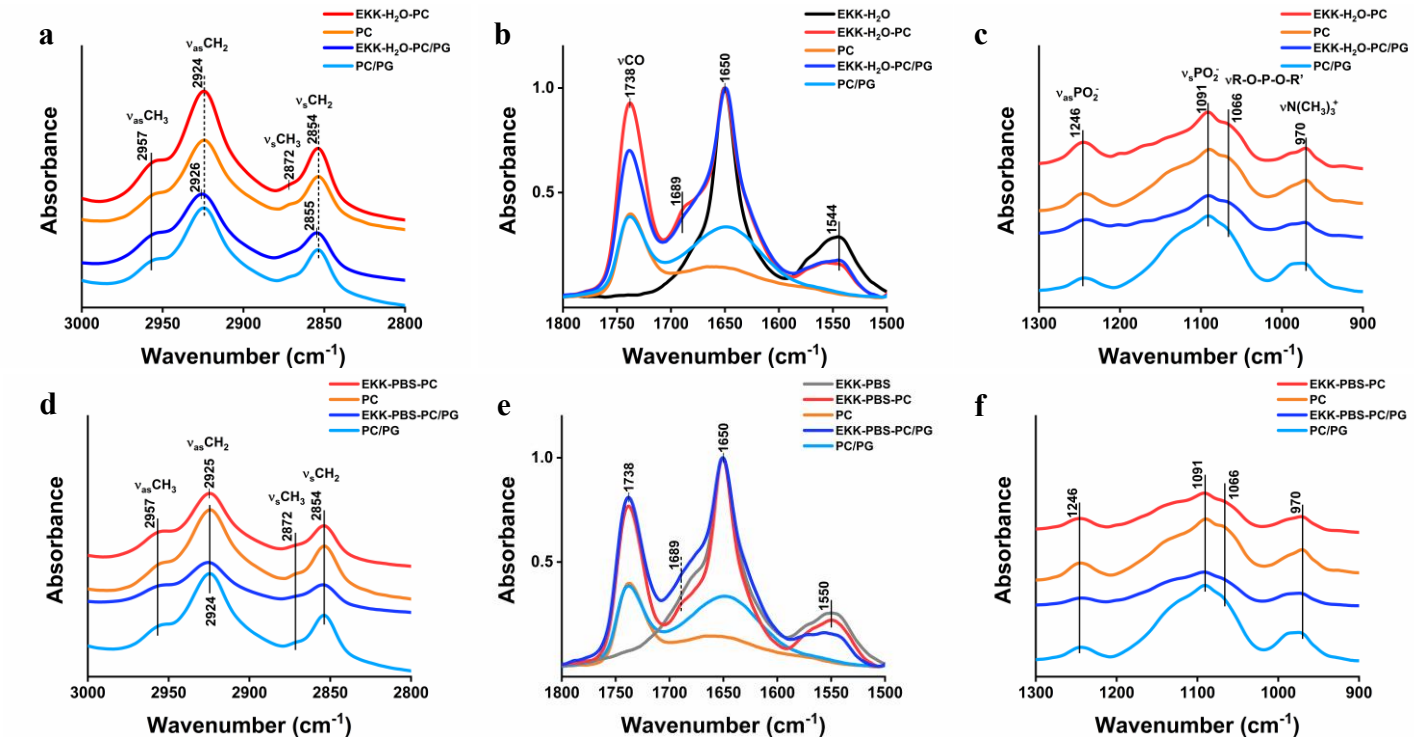

Supplementary Figure 9: IR spectra of EKK (125 μM) in presence of liposome in water (ratio EKK:liposome, 1:10) in: a) acyl region, b) amide region, c) phosphate region. EKK (125 μM) in presence of liposome in PBS (ratio EKK:liposome, 1:10) in d) acyl region, e) amide region, f) phosphate region. Significant shifts are indicated in the acyl region of the PC/PG liposome in water.

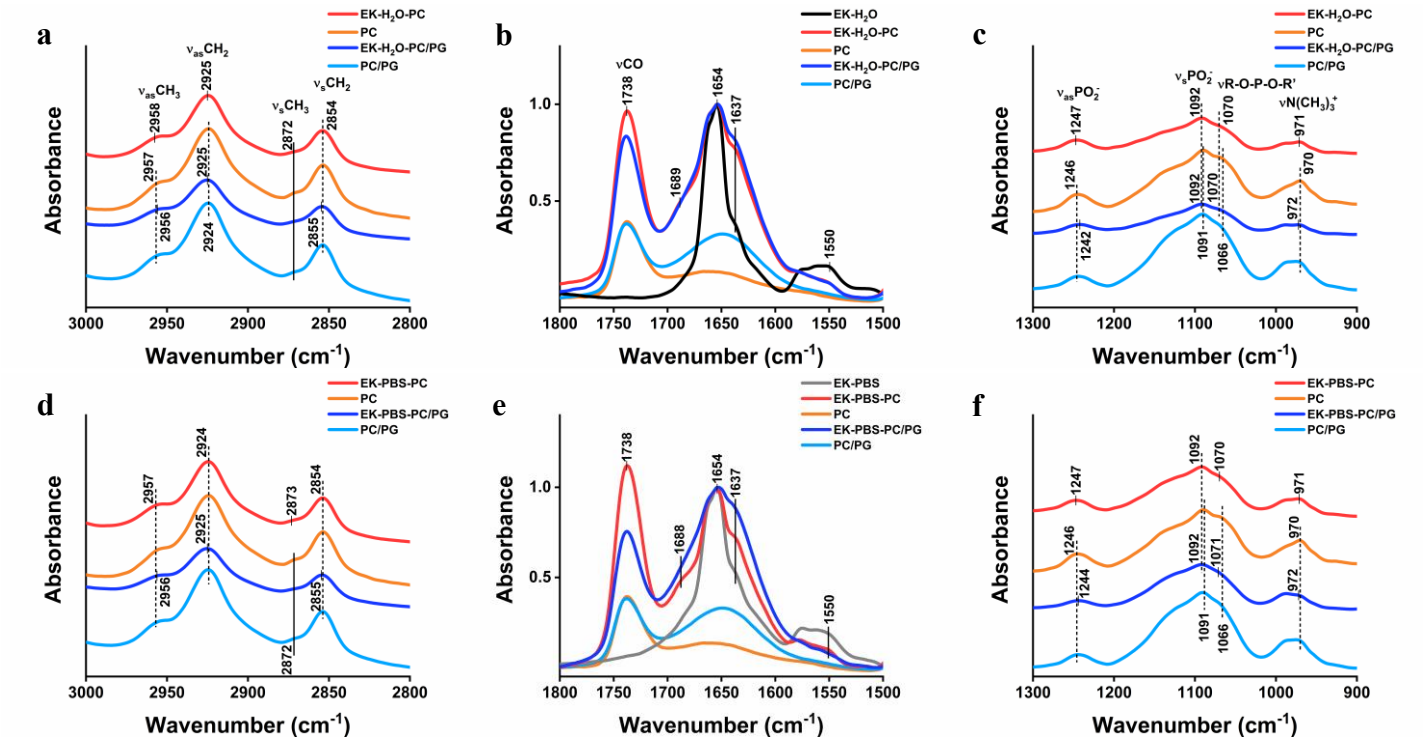

Supplementary Figure 10: IR of EK (125 μM) in presence of liposome in water (ratio EK:liposome, 1:10) in: a) acyl region, b) amide region, c) phosphate region. EK (125 μM) in presence of liposome in PBS (ratio EK:liposome, 1:10) in d) acyl region, e) amide region, f) phosphate region. Significant shifts are indicated in the acyl region.

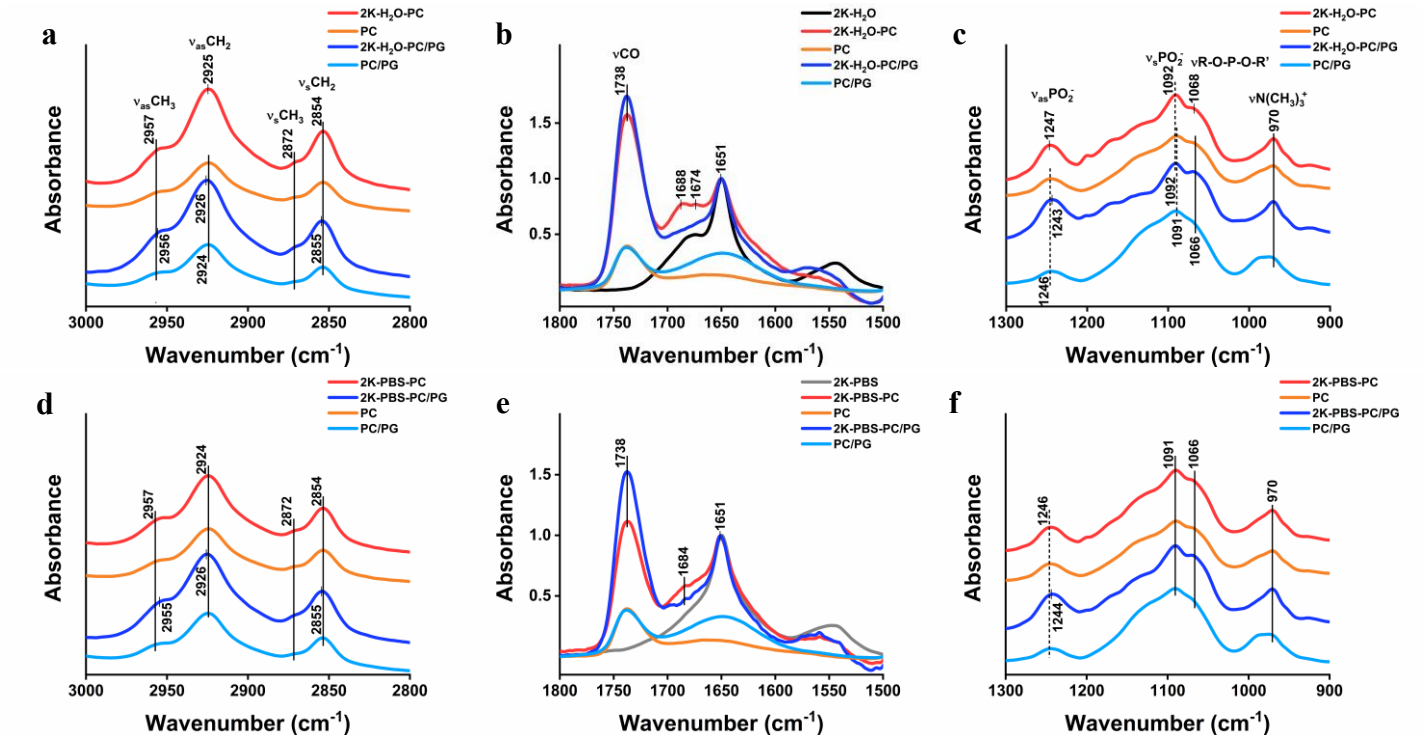

Supplementary Figure 11: IR of 2K (125 μM) in presence of liposome in water (ratio 2K:liposome, 1:10) in: a) acyl region, b) amide region, c) phosphate region. 2K (125 μM) in presence of liposome in PBS (ratio 2K:liposome, 1:10) in d) acyl region, e) amide region, f) phosphate region. Significant shifts are indicated in the acyl region.

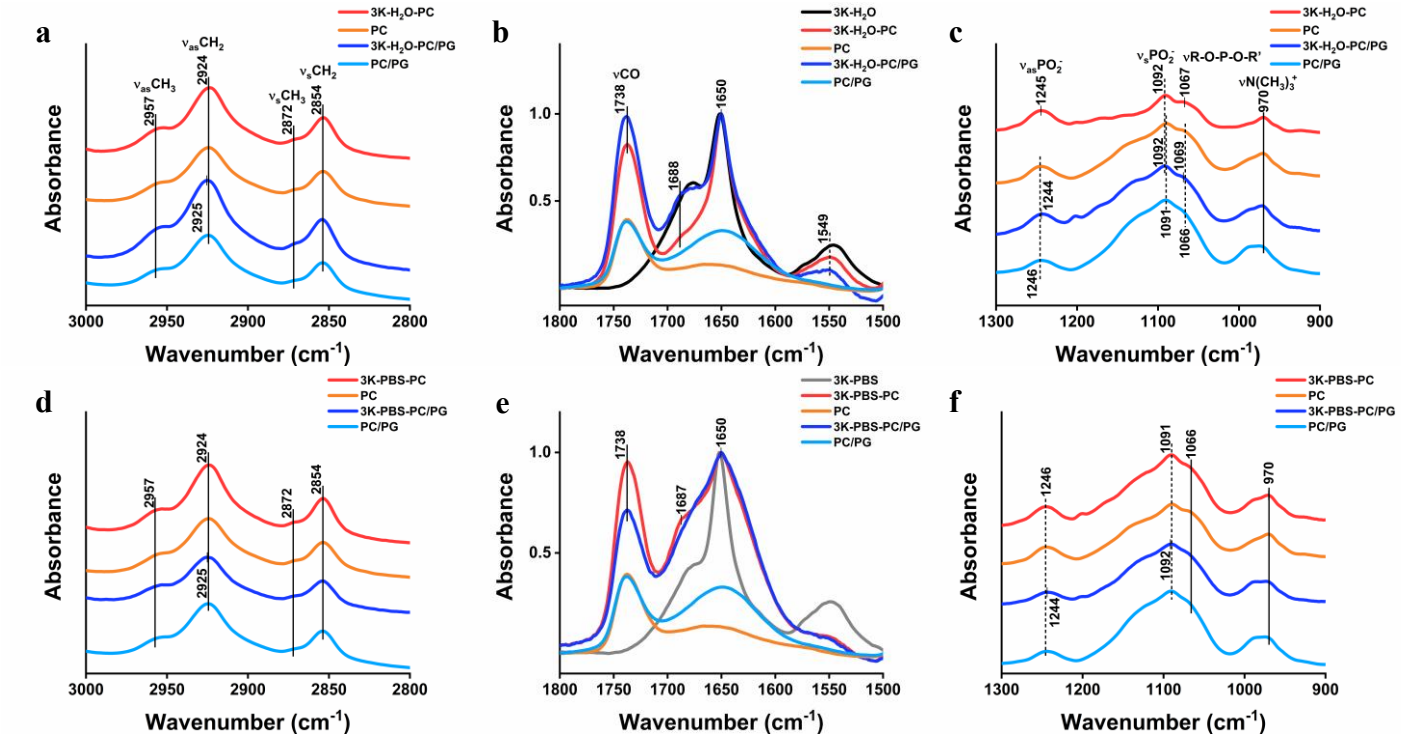

Supplementary Figure 12: IR of 3K (125 μM) in presence of liposome in water (ratio 3K:liposome, 1:10) in: a) acyl region, b) amide region, c) phosphate region. 3K (125 μM) in presence of liposome in PBS (ratio 3K:liposome, 1:10) in d) acyl region, e) amide region, f) phosphate region.

Zeta potential

Zeta potential measurements were conducted on liposomes composed of PC and PC/PG in both water and PBS media. The liposomes were tested in the presence of EKK and 3K at the initial concentration of 125 μM

(Supplementary Table 3). To facilitate a comprehensive analysis and comparison, the liposomes were examined across four systems (PC in water, PC/PG in water, PC in PBS and PC/PG in PBS), featuring well-known cationic antimicrobial peptides with charges ranging from 0 to +6, as presented in Supplementary Table 4. p53(17-26), a neutral anticancer peptide fragment was selected as negative control to understand the effect of charge while CM15 carries +6 charge and used as cationic control. Aurein 1.2 and dermicidin were selected as charge representative of EKK and 3K respectively.

The neutral peptide p53 did not significantly alter the negative zeta potential in both liposome systems irrespective of the media which is consistent with our recent study where the effects of peptides aurein 1.2, dermicidin, and p53 on red blood cell-derived extracellular vesicles (REVs) were studied.[10] Dermicidin caused a slight decrease in the magnitude of negative zeta potential with liposome which is also consistent with the recent REVs results. However, aurein 1.2 (a peptide with a net charge of +1) significantly reduced the magnitude of the negative zeta potential of liposome upon interaction, aligning with our previous results, where 125 µM led to near-zero values and charge reversal, except in the case of PC/PG in PBS. The changes in zeta potential observed for aurein 1.2 and dermcidin indicate that the action is not solely charge-dependent but also mechanism-dependent as observed in the study with REVs.[10] Furthermore, for all four peptides, supramolecular formation appears to be a crucial factor.

Supplementary Table 3: Zeta potential changes of liposomes PC and PC/PG in water and PBS media upon addition of EKK and 3K. A concentration ratio of peptide-to-liposome of 1:10 was maintained for model membranes.

Sample	**Zeta potential (mV)**
PC in water (PC-H_2O)	-34.5 ± 8.94
EKK-H_2O-PC	-32.5 ± 3.59
3K-H_2O-PC	-17 ± 4.22
PC/PG-H_2O	-66.4 ± 20.1
EKK-H_2O-PC/PG	-50.8 ± 6.71
3K-H_2O-PC/PG	-50.9 ± 12.5
PC-PBS	-27.3 ± 13.6
EKK-PBS-PC	-18.5 ± 3.91
3K-PBS-PC	-27 ± 6.68
PC/PG-PBS	-65.4 ± 13.6
EKK-PBS-PC/PG	-48.4 ± 8.91
3K-PBS-PC/PG	-85.9 ± 8.14

Supplementary Table 4: Zeta potential changes of liposomes PC and PC/PG in water and PBS media upon addition of selected peptides. The net charge values of the supplemented peptides are listed. A concentration ratio of peptide-to-liposome of 1:10 was maintained for model membranes

Sample	**Zeta potential (mV)**	**Net charge of the added peptide**
PC-H_2O	-32.8 ± 8.54	zwitterionic
p53(17-26)-H_2O-PC	-32 ± 0.36	0
Aurein1.2-H_2O-PC	1 ± 5.38	+1
Dermicidin-H_2O-PC	-24.8 ± 0.75	+3
CM15-H_2O-PC	-17.3 ± 5.3	+6
PC/PG-H_2O	-63.4 ± 18.8	Negative
p53(17-26)-H_2O-PC/PG	-56.4 ± 15.2	0
Aurein1.2-H_2O-PC/PG	-0.35 ± 2.24	+1
Dermicidin-H_2O-PC/PG	-45.8 ± 11.3	+3
CM15- H_2O -PC/PG	-15.8 ± 4.03	+6
PC-PBS	-27.8 ± 13.6	zwitterionic
p53(17-26)-PBS-PC	-25.76 ± 7.76	0
Aurein1.2-PBS-PC	-0.48 ± 2.67	+1
Dermicidin-PBS-PC	-18.6 ± 2.38	+3
CM15-PBS-PC	-12.36 ± 6.05	+6
PC/PG-PBS	-58.6 ± 10.53	Negative
p53(17-26)-PBS-PC/PG	-51.3 ± 7.57	0
Aurein1.2-PBS-PC/PG	-57.65 ± 11.2	+1
Dermicidin-PBS-PC/PG	-54.83 ± 14.3	+3
CM15-PBS-PC/PG	0.9 ± 0.95	+6

Supplementary Table 5: Hemolytic activity of the peptides tested on human red blood cells in PBS. Peptides were tested on human red blood cells (1% (*V/V*)) and based on the dose-response curves after fitting with non-linear regression on the hemolysis percentage, HC_{50} values were determined. The data are represented as mean ± SD, N = 4.

Peptides	HC_{50} [µM] ± SD
EK	92.04 ± 8.21
EKK	> 250
2K	103 ± 5.12
3K	29.82 ± 1.26

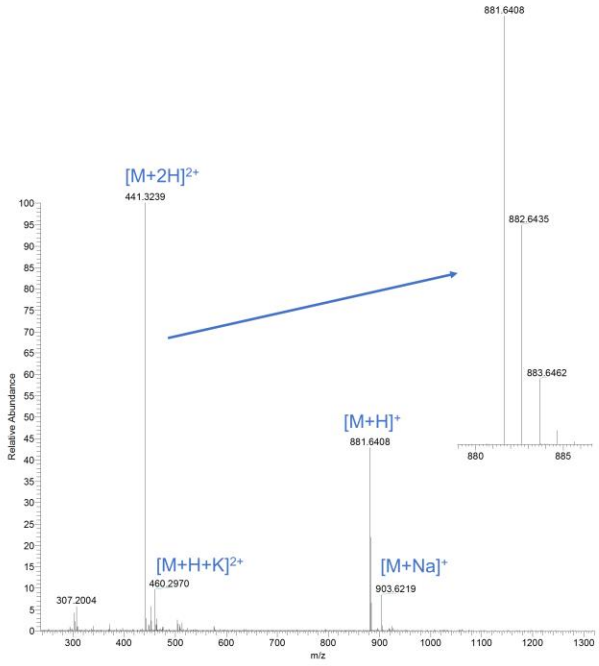

Supplementary Figure 13: High resolution mass spectrum of EK. The observed monoisotopic molecular mass is 880.6335. Calcd. M_{mo} = 880.6361; Δppm = 2.95.

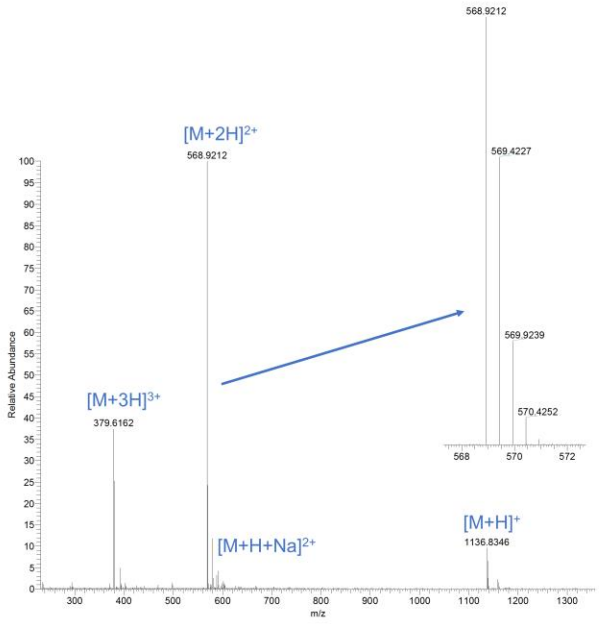

Supplementary Figure 14: High resolution mass spectrum of EKK. The observed monoisotopic molecular mass is 1135.8278 Da. Calcd. M_{mo} = 1135.8308; Δppm = 2.64.

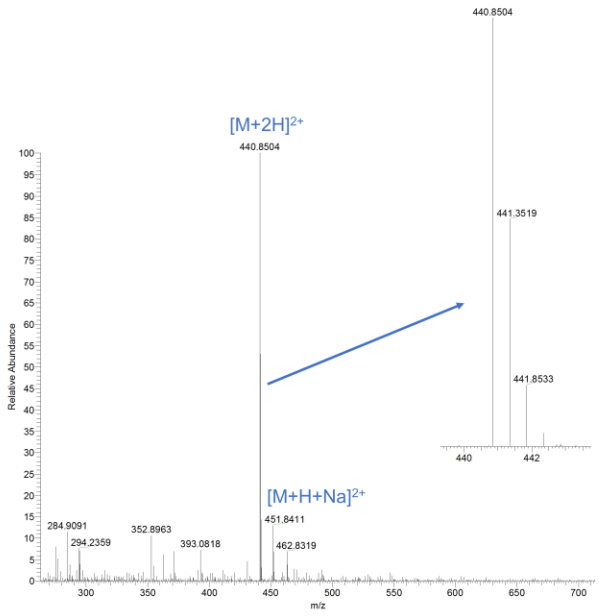

Supplementary Figure 15: High resolution mass spectrum of 2K. The observed monoisotopic molecular mass is 879.6862 Da. Calcd. M_{mo} = 879.6885; Δppm = 2.61.

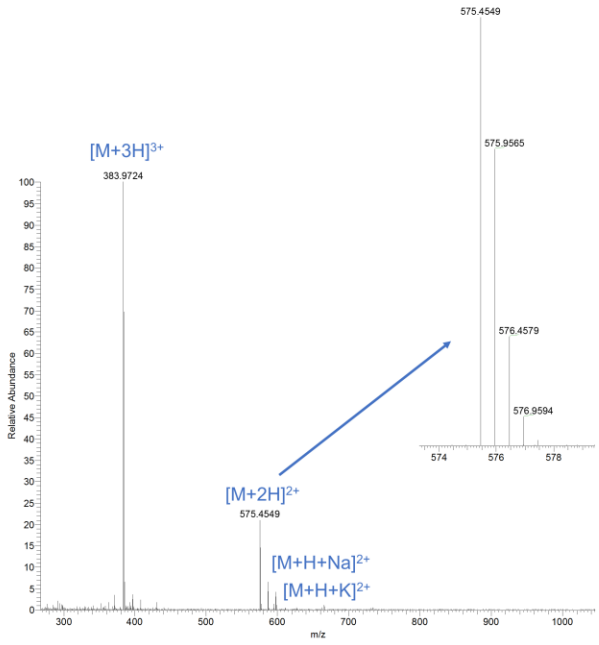

Supplementary Figure 16: High resolution mass spectrum of 3K. The observed monoisotopic molecular mass is 1148.8954. Calcd. M_{mo} = 1148.8988; Δppm = 2.99.

1 M. Quemé-Peña, T. Juhász, J. Mihály, I. Cs. Szigyártó, K. Horváti, S. Bősze, J. Henczkó, B. Pályi, C. Németh, Z. Varga, F. Zsila and T. Beke-Somfai, *ChemBioChem*, 2019, **20**, 1578–1590.

2 F. Zsila, S. Bösze, K. Horváti, I. C. Szigyártó and T. Beke-Somfai, *RSC Adv.*, 2017, **7**, 41091–41097.

3 A. Kitamura, T. Kiyota, M. Tomohiro, A. Umeda, S. Lee, T. Inoue and G. Sugihara, *Biophys. J.*, 1999, **76**, 1457–1468.

4 I. C. Szigyártó, J. Mihály, A. Wacha, D. Bogdán, T. Juhász, G. Kohut, G. Schlosser, F. Zsila, V. Urlacher, Z. Varga, F. Fülöp, A. Bóta, I. Mándity and T. Beke-Somfai, *Chem. Sci.*, 2020, **11**, 6868–6881.

5 J. W. Brauner, R. Mendelsohn and F. G. Prendergast, *Biochemistry*, 1987, **26**, 8151–8158.

6 M. Quemé-peña, T. Juhász, G. Kohut, M. Ricci, P. Singh, I. C. Szigyártó, Z. I. Papp, L. Fülöp and T. Beke-somfai, *Int. J. Mol. Sci.*, DOI:10.3390/ijms22168613.

7 A. Bóta, A. Wacha, Z. Varga, I. C. Szigyártó, S. Kristyán, A. Lőrincz, P. Szabó, M. Kálmán, L. Naszályi-Nagy and J. Mihály, *J. Colloid Interface Sci.*, 2018, **532**, 782–789.

8 A. Lőrincz, J. Mihály, A. Wacha, C. Németh, B. Besztercei, P. Gyulavári, Z. Varga, I. Peták and A. Bóta, *Mater. Sci. Eng. C*, DOI:10.1016/j.msec.2021.112481.

9 A. Arouri, M. Dathe and A. Blume, *Biochim. Biophys. Acta - Biomembr.*, 2009, **1788**, 650–659.

10 T. Sonallya, T. Juhász, I. C. Szigyártó, K. Ilyés, P. Singh, D. Khamari, E. I. Buzás, Z. Varga and T.